Inorganic Chemistry

Article

pubs.acs.org/IC

# Cooperative Effects of Electron Donors and Acceptors for the Stabilization of Elusive Metal Cluster Frameworks: Synthesis and Solid-State Structures of $[Pt_{19}(CO)_{24}(\mu_4\text{-}AuPPh_3)_3]^-$ and $[Pt_{19}(CO)_{24}\{\mu_4\text{-}Au_2(PPh_3)_2\}_2]$

Alessandro Ceriotti,*[,†] Piero Macchi,*[,‡] Annalisa Sironi,[§] Simona El Afefey,[†,⊥] Matteo Daghetta,[∥] Serena Fedi,[⊥] Fabrizia Fabrizi de Biani,[⊥] and Roberto Della Pergola[§]

[†]Dipartimento di Chimica, Università degli Studi di Milano, via Golgi 19, 20133 Milano, Italy

[‡]Department of Chemistry and Biochemistry, University of Bern, Freiestrasse 3, 3012 Bern, Switzerland

[§]Dipartimento di Scienze dell'Ambiente e del Territorio, Università di Milano—Bicocca, piazza della Scienza 1, 20126 Milano, Italy

[⊥]Dipartimento di Chimica, Università degli Studi di Siena, via Aldo Moro, 53100 Siena, Italy

[∥]Dipartimento di Chimica, Materiali e Ingegneria Chimica "Giulio Natta", Politecnico di Milano, Piazza L. Da Vinci 32, 20133 Milano, Italy

Supporting Information

**ABSTRACT:** The anionic cluster $[Pt_{19}(CO)_{22}]^{4-}$ (**1**), of pentagonal symmetry, reacts with CO and $AuPPh_3^+$ fragments. Upon increasing the Au:$Pt_{19}$ molar ratio, different species are sequentially formed, but only the last two members of the series could be characterized by X-ray diffraction, namely, $[Pt_{19}(CO)_{24}(\mu_4\text{-}AuPPh_3)_3]^-$ (**2**) and $[Pt_{19}(CO)_{24}\{\mu_4\text{-}Au_2(PPh_3)_2\}_2]$ (**3**). The metallic framework of the starting cluster is completely modified after the addition of CO and $AuL^+$, and both products display the same platinum core of trigonal symmetry, with closely packed metal atoms. The three $AuL^+$ units cap three different square faces in **2**, whereas four $AuL^+$ fragments are grouped in two independent bimetallic units in the neutral cluster **3**. Electrochemical and spectroelectrochemical studies on **2** showed that its redox ability is comparable with that of the homometallic **1**.

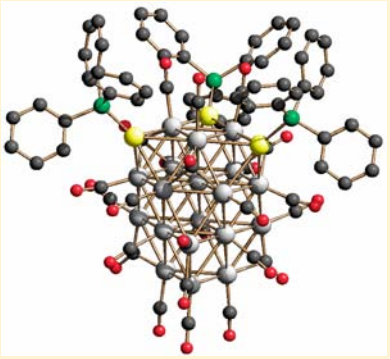

## INTRODUCTION

Many Pt−Au mixed-metal clusters have been obtained in the past, and most of them contain three to six metal atoms. These compounds have assumed particular relevance because of their peculiar bonding properties.[1] In the field of high-nuclearity clusters (Pt + Au > 6), few examples are known, either rich in Pt[2] or with a high Au content.[3] A few trimetallic clusters, mainly containing other metals of groups 11 and 12 (Cu, Ag, and Hg), were also reported,[4] and they are typically based on icosahedral structures. Besides theoretical and structural aspects, the combination of Pt and Au in molecular compounds of well-defined composition may be relevant for the preparation of bimetallic nanoparticles, which are known to possess excellent activity in electrocatalysis,[5] and for the catalytic oxidation of glycerol.[6]

The anion $[Pt_{19}(CO)_{22}]^{4-}$ (**1**) has played a special role in the field of carbonyl clusters because it remained for a long time the largest structurally characterized compound of this kind. Moreover, it is still one of the rare examples of high-nuclearity carbonyl clusters possessing a framework of pentagonal symmetry.[7] Despite these peculiarities, the studies on its reactivity were hampered by the difficult characterization of the fairly unstable products. For example, it is known that the reactions of **1** with $NO^+$ and $H^+$ eventually lead to the formation of $[Pt_{38}(CO)_{44}]^{2-}$, but only $[Pt_{19}(CO)_{21}NO]^{3-}$ could be isolated as an intermediate.[8] Nevertheless, some electrochemical investigations have been described, showing that the cluster undergoes several couples of redox processes, spanning reversibly the 8−/0 oxidation states.[9]

One of us deeply investigated the behavior of the cluster under a carbon monoxide (CO) atmosphere, observing a clean, quantitative, and rapid reaction, but also in this case, the real nature of the product could never be ascertained. In contrast to what is normally observed,[10] the IR bands of the carbonylated product shift to *lower* wavenumbers, indicating an increased metal-to-ligand back-donation and suggesting that this uncharacterized species would be a better electron donor toward electrophiles.

For all of these reasons, in order to verify the donor properties of the carbonylated product and to compare them with those of **1**, we performed new experiments, aiming at the

**Received:** October 18, 2012
**Published:** January 30, 2013

   dx.doi.org/10.1021/ic302282y | *Inorg. Chem.* 2013, 52, 1960−1964

stable addition of gold electrophilic fragments. The first results in this field, namely, the chemical and structural characterization of Pt−Au heterometallic clusters, are described here. In sharp contrast with the pentagonal symmetry of **1** and other heterometallic compounds, the metallic frameworks of $[Pt_{19}(CO)_{24}(\mu_4\text{-}AuPPh_3)_3]^-$ (**2**) and $[Pt_{19}(CO)_{24}\{\mu_4\text{-}Au_2(PPh_3)_2\}_2]$ (**3**) are rare examples of close-packed Pt−Au metal clusters stabilized by the cooperative effect of the electron-donor Au fragment and the electron-acceptor CO ligand.

## RESULTS

**Synthesis and Reactivity.** The reaction of **1** with $PPh_3AuCl$ was carried out in acetonitrile at ambient temperature, under CO, or under an inert atmosphere: in both cases, IR monitoring of the reaction mixture showed systematic trends: (i) upon the addition of the Au complex, a progressive shift of the CO bands to higher wavenumbers was observed; (ii) at the same Au:$Pt_{19}$ molar ratios, the products formed under CO had IR maxima red-shifted about 10 $cm^{-1}$ with respect to the products formed under an inert atmosphere.

Under CO, when the Au:$Pt_{19}$ molar ratio is 3:1, a brown precipitate forms, which can be easily isolated by filtration and dissolved in tetrahydrofuran (THF) for characterization and crystallization. This species is stable under an inert atmosphere and does not need to be handled under CO. Thus, crystals of $(NBu_4)[Pt_{19}(CO)_{24}(AuPPh_3)_3][(NBu_4)\mathbf{2}]$ suitable for X-ray determination were obtained by layering this THF solution with 2-propanol.

The low solubility of the salts of **2** in acetonitrile hampered further reactions with an excess of $PPh_3AuCl$. Therefore, in order to obtain clusters with a higher Au content, we reacted THF solutions of pure **2** with the solvated cationic complex $[PPh_3AuTHF]^+$, obtained in situ from $PPh_3AuCl$ and $Ag^+$.

This reaction induced a definite shift of the IR carbonyl bands and allowed isolation of the neutral cluster **3** by precipitation with 2-propanol.

Thus, the whole series of reactions can be summarized with the following chemical equations:

$$[Pt_{19}(CO)_{22}]^{4-}\ [\nu(CO)\ 2005s,\ 1930sh,\ 1799m\ cm^{-1}] + 2CO \rightarrow [Pt_{19}(CO)_{24}]^{4-}\ [\text{not isolated},\ \nu(CO)\ 1996s,\ 1928sh,\ 1801w,\ br,\ 1752m\ cm^{-1}]$$

$$[Pt_{19}(CO)_{24}]^{4-} + 3AuPPh_3Cl \rightarrow [Pt_{19}(CO)_{24}(AuPPh_3)_3]^- + 3Cl^-$$

$$[Pt_{19}(CO)_{24}(AuPPh_3)_3]^- + [PPh_3AuTHF]^+ \rightarrow [Pt_{19}(CO)_{24}\{\mu_4\text{-}Au_2(PPh_3)_2\}_2]$$

$^{31}P\{^1H\}$ NMR spectra have been recorded for both clusters in acetone-$d_6$ at 183 K, but only for $(PPh_4)\mathbf{2}$ we could detect a signal, consisting of a sharp singlet ($PPh_4^+$) and a few narrow lines emerging from a broad band centered at 67 ppm. Even assuming a $^3J(^{31}P-^{195}Pt)$ value close to zero, a very complex spectrum could be anticipated because the $P_3Au_3Pt_9$ unit is a 12-spin system, with many magnetically inequivalent isotopomers, corresponding to the different clusters with zero to nine NMR-active $^{195}Pt$ ($S = {}^1/_2$; natural abundance 34%). Therefore, it was impossible to estimate the $^2J(^{31}P-^{195}Pt)$ value and to compare it with the few values reported for $AuPPh_3$ units bonded to Pt in carbonyl clusters, ranging from 500 to 300 Hz.[4,11] The absence of any signal in the $^{31}P$ NMR spectrum of **3** can be a consequence of its limited solubility or of dynamic processes involving the four $AuPPh_3$ groups. Besides dissociation, two additional processes can be envisaged, involving the exchange of nonequivalent Au sites within the two $Au_2$ units, and scrambling of the $Au_2$ entities over the three square faces available. Indeed, $Au_2(PR_3)_2$ moieties in carbonyl clusters are known to be highly fluxional.[12]

**Crystal Structures.** The solid-state structure of **2**, including all of the carbonyl and phosphine ligands, is shown in Figure 1; the atom labeling of the metallic framework of **3** is reported in Figure 2; their relevant structural parameters are compared in Table 1.

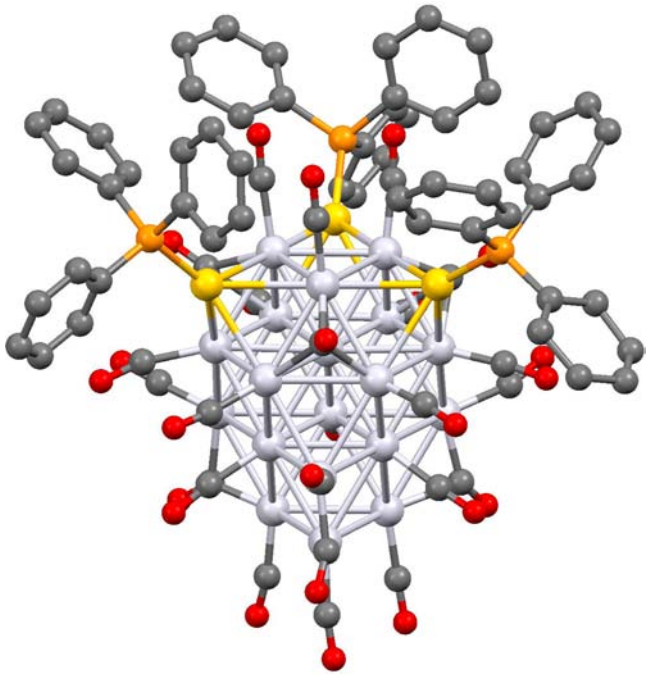

**Figure 1.** Solid-state structure of **2** from X-ray diffraction refinements.

The platinum framework is identical in the two compounds, being composed of a closed-packed face-centered-cubic core and four layers of three, seven, six, and three atoms, respectively. All Pt atoms but one are located on the surface and bear at least one carbonyl ligand, whereas Pt1 is fully interstitial at the center of the second layer. The cluster can be idealized as a cubic octahedron, with three square faces capped by another three Pt atoms and face-fused with an octahedron (see Figure 2). The upper part of the cluster is therefore exposing three square faces and four triangular faces as a cubic octahedron. The two structures differ, however, in the coordination of $AuPPh_3$: in **2**, the three fragments are all capping three square faces, whereas in **3**, they form two $(AuPPh_3)_2$ dumbbells that asymmetrically cap one square face. The distribution of the carbonyl ligands is similar in **2** and **3**. Thus, the ideal symmetry is $C_s$ in **3** and $C_{3v}$ in **2** (reduced to $C_1$ and $C_3$, respectively, if the out-of-plane rotation of the phenyl rings is considered). In the crystal structures, **2** is mirror-symmetric, whereas **3** is not sitting on any symmetry element.

The Pt−Au bond distances in **2** span the range 2.80−2.93 Å and average 2.86 Å. They are systematically longer for the three Pt3 atoms of the outer triangle (>2.85 Å) and shorter for the


dx.doi.org/10.1021/ic302282y | Inorg. Chem. 2013, 52, 1960−1964

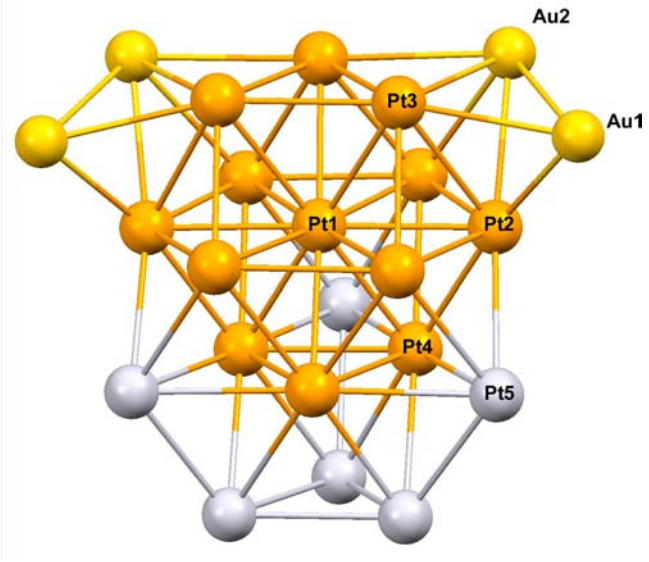


**Figure 2.** Metallic framework of **3**. The $Pt_{13}$ cubic octahedron core is highlighted in orange. The remaining Pt atoms are in light gray and the four Au atoms in yellow.

**Table 1. Averaged Pt−Pt Distances (in Å) in the Cores of the Two Clusters**[a]

| Pt−Pt bond | no. of bonds | **2** | **3** |
|---|---|---|---|
| Pt1−Pt2 | 6 | 2.796(6) | 2.79(4) |
| Pt1−Pt3 | 3 | 2.82(2) | 2.81(8) |
| Pt1−Pt4 | 3 | 2.77(1) | 2.76(4) |
| Pt2−Pt2 | 6 | 2.79(2) | 2.79(5) |
| Pt2−Pt3 | 6 | 2.76(1) | 2.79(5) |
| Pt2−Pt4/Pt5 | 12 | 2.80(1) | 2.79(5) |
| Pt3−Pt3 | 3 | 2.81(2) | 2.81(3) |
| Pt4/Pt5−Pt4/Pt5 | 9 | 2.833(8) | 2.822(5) |

[a]Numbers in parentheses are the standard deviations from the mean.

Pt2 atoms of the inner hexagon (<2.85 Å), suggesting a slightly stronger interaction. In **3** the Pt−Au distances are more scattered, being included in the range 2.64 −2.97 Å, but the average (2.84 Å) is almost unchanged. The shorter distances are those connecting the two more external Au1 atoms, bound to only two Pt atoms (see Figure 2).

In both crystal structures, the clusters leave large voids to host solvent molecules and cations (in **2**) which are not visible, given the relative scarce diffraction and the likely disordered arrangement around the clusters.

**Electrochemical Studies.** As illustrated in Figure 3, $(PPh_4)$**2** undergoes one anodic process at +0.45 V, complicated by subsequent chemical reactions. In fact, we are in the presence of an ECE mechanism with the formation of a byproduct undergoing two new oxidation processes at +0.73 and +0.88 V. By analogy with what has been observed for the series $[Pt_{19}(CO)_{22}]^{4-}$, $[Pt_{24}(CO)_{30}]^{2-}$, and $[Pt_{38}(CO)_{44}]^{2-}$, two pairs of cathodic processes, separated by ∼300 mV, are also visible at −0.31, −0.65, −1.66, and −1.90 V, only the first of which manifesting features of chemical reversibility in the time scale of cyclic voltammetry (CV). In fact, at lower scan rates, the departure from the current ratio $i_{p(reverse)}/i_{p(forward)} = 1$ expected for a chemical reversible process is observed for all of the reduction steps, except for the first. A fifth reduction process at −2.25 V is also detected, while the possible partner of this pair

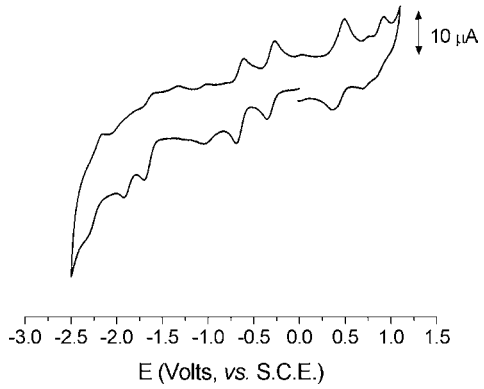


**Figure 3.** CV profile recorded at a platinum electrode in a THF solution of $(PPh_4)$**2** ($0.5 \times 10^{-3}$ M): supporting electrolyte, $(NBu_4)PF_6$ (0.2 M); scan rate, 0.2 V $s^{-1}$.

could be beyond the experimental window, limited by solvent discharge. Controlled-potential coulometric tests in correspondence with the first reduction ($E_w$ = −0.4 V) proved that it involves one electron per molecule, while CV on the exhaustively reduced solution indicates that also the addition of one electron, in fact, causes partial decomposition of the cluster, as suggested by the appearance of new small peaks and by the general decrease of the current intensity.

In spite of the incomplete stability of the electrogenerated neutral and dianionic species, we have monitored by IR spectroelectrochemistry the variation of $\nu$(CO) of both the terminal and bridging groups of this cluster. The experiment has been conducted in situ step-by-step, in order to maintain the isosbestic points, so that electrolysis was, in fact, not completed. As expected, in both cases, the original spectrum is only partially recovered on the backscan. Figure 4 illustrates the IR spectral trend recorded in the 0/1− and 1−/2− passage.

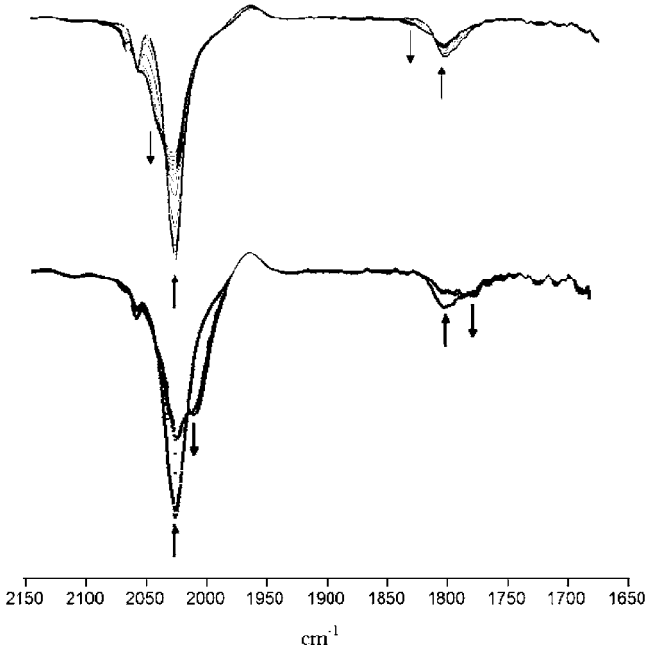


**Figure 4.** IR spectral changes recorded in an optically transparent thin-layer electrode cell upon the progressive oxidation (top) and reduction (bottom) of **2**: THF solution; supporting electrolyte, $(NBu_4)PF_6$ (0.2 M).


dx.doi.org/10.1021/ic302282y | Inorg. Chem. 2013, 52, 1960−1964

The original spectrum shows two main absorptions: at 2027 $cm^{-1}$, which is assigned to the stretching vibration of the carbonyl groups terminally bound at the metal core, and at 1803 $cm^{-1}$, which is assigned to the stretching vibration of the bridging carbonyl groups. Upon oxidation, both bands are blue-shifted by ∼15−20 $cm^{-1}$ and appear at 2042 and 1821 $cm^{-1}$, while the contrary happens upon reduction, with two new bands appearing at 2009 and 1780 $cm^{-1}$. This is a common trend followed by carbonyl clusters and indicates decreasing or increasing d$\pi$-Pt → $\pi^*$-CO back-bonding induced by electron removal or addition, respectively. It is interesting to note the agreement between the $\nu$(CO) trend and the first oxidation or first reduction redox potential values of the pristine sample of **2** compared to the analogous values observed for $[Pt_{19}(CO)_{22}]^{4-}$ (2001 $cm^{-1}$ and −0.15 and −1.13 V, for the first oxidation and first reduction, respectively).[8] All of these values clearly indicate how the $\{Pt_{19}^{4-}\}$ metallic core is much less electron-rich in **2** than in the parent **1**.

As illustrated in Figure 5, the redox behavior of the neutral cluster **3** seems somehow reminiscent of that of **2** because an

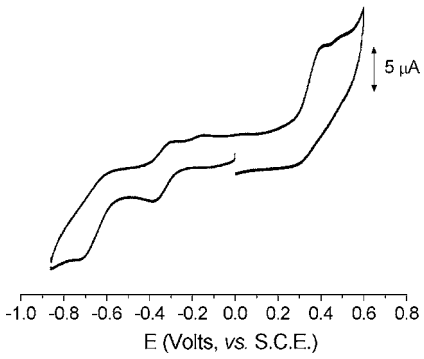


**Figure 5.** CV profile recorded at a platinum electrode in a THF solution of **3** ($0.4 \times 10^{-3}$ M): supporting electrolyte, $(NBu_4)PF_6$ (0.2 M); scan rate, 0.2 V $s^{-1}$.

oxidation ($E^\circ$ = +0.33 V) and a couple of reductions (at $E^\circ$ = −0.34 and −0.67 V) are observed. A clear trait of the illustrated CV is the general lower chemical reversibility of all of these redox processes ($i_{p(reverse)}/i_{p(forward)}$ at $\nu$ = 0.2 V $s^{-1}$ is 0.1 for the oxidation and 0.5 and 0.2 for the first and second reductions, respectively). Anyway, a closer inspection of the redox pattern of **3**, obtained by using a potential step technique, like, for example, differential pulse voltammetry (DPV) shown in Figure 6, reveals a more complicated situation. In fact, the presence of

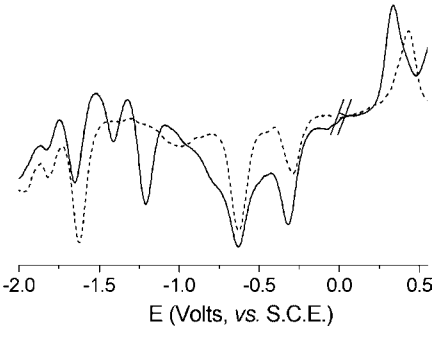


**Figure 6.** DPV responses recorded at a platinum electrode in a THF solution of **2** ($0.5 \times 10^{-3}$ M, dashed line) and **3** ($0.4 \times 10^{-3}$ M, full line): supporting electrolyte, $(NBu_4)PF_6$ (0.2 M).

a mixture of **2** and **3** is clearly revealed. A new couple of anodic processes is visibly detectable at −1.21 and −1.41 V, so it is questionable whether the true first couple of anodic processes of **3** is partially hidden by the correspondent couple of anodic processes of **2**. As a matter of fact, two shoulders at −0.53 and −0.78 V are visible behind the first couple of reductions of **2**, which could be possibly ascribed to **3**. The low solubility and redox instability of **3** probably prevent a more correct interpretation. In conclusion, as a general trend, the addition of heterometallic Au fragments reduces the electron content of these Pt clusters and, at the same time, makes them much less prone to the electron-sink behavior observed for the homometallic related family of clusters.

## EXPERIMENTAL SECTION

All of the solvents were purified and dried by conventional methods and stored under nitrogen. All of the reactions were carried out under an oxygen-free nitrogen atmosphere using the Schlenk-tube technique.[13] $(PPh_4)_4[Pt_{19}(CO)_{22}]$[6] and $PPh_3AuCl$[14] were prepared by literature methods. IR spectra in solution were recorded on a Nicolet Avatar 360 FT-IR spectrophotometer, using calcium fluoride cells previously purged with dinitrogen. Elemental analyses were carried out by the staff of Laboratorio di Analisi of the Dipartimento di Chimica.

CV was performed in a three-electrode cell containing a gold or a glassy carbon working electrode surrounded by a platinum spiral counter electrode and an aqueous saturated calomel reference electrode (SCE) mounted with a Luggin capillary. A BAS 100W electrochemical analyzer was used as the polarizing unit. All of the potential values are referred to the SCE. Under the present experimental conditions, the one-electron oxidation of ferrocene occurs at $E^{\circ\prime}$ = +0.38 V in an acetonitrile solution and $E^{\circ\prime}$ = +0.59 V in a THF solution. Controlled-potential coulometry was performed in an H-shaped cell with anodic and cathodic compartments separated by a sintered-glass disk. The working macroelectrode was a platinum gauze; a mercury pool was used as the counter electrode.

Anhydrous 99.8% acetonitrile was an Aldrich product. Anhydrous 99.9% HPLC-grade THF (Aldrich) was distilled in the presence of sodium before use. Fluka $(NBu_4)PF_6$ or $(NEt_4)PF_6$ (electrochemical grade) were used as supporting electrolytes.

$^{31}P\{^1H\}$ NMR spectra have been recorded on a 300 MHz Bruker spectrometer, operating at 121.5 MHz and referenced to $H_3PO_4$ in $D_2O$.

**Synthesis of 2.** A total of 720 mg (0.127 mmol) of $(PPh_4)_4[Pt_{19}(CO)_{22}]$ was dissolved with 20 mL of $CH_3CN$ in a Schlenk tube; the brown solution was put under a CO atmosphere and stirred for 1 h. Solid $PPh_3AuCl$ (188 mg, 0.381 mmol) was then added in three subsequent portions. The solution was stirred overnight. A brown powder gradually separated. It was recovered by filtration, washed with 2-propanol (2 × 10 mL), and dried in a vacuum. $\nu$(CO) (THF): 2059w, 2027s, 1804w $cm^{-1}$. Yield: 515 mg (66%). Elem. anal. Found: C, 20.8; H, 1.20. Calcd: C, 20.10; H, 1.07.

$(NBu_4)$**2** used for X-ray diffraction was prepared analogously from $(NBu_4)_4[Pt_{19}(CO)_{22}]$ with comparable yields. Crystals were grown from THF/2-propanol. Elem. anal. Found: C, 18.91; H, 1.53; N, 0.51. Calcd: C, 18.81; H, 1.35; N, 0.23.

**Synthesis of 3.** A solution of $(PPh_4)$**2** (264 mg, 0.043 mmol) in 25 mL of THF was stirred under a CO atmosphere. In another Schlenk tube, $PPh_3AuCl$ (22 mg, 0.044 mmol) and $AgBF_4$ (9 mg, 0.046 mmol) were mixed in 1 mL of THF, giving rise to a fine white powder (AgCl), which was decanted. The colorless solution of $[PPh_3AuTHF]BF_4$ was added in small subsequent portions to the cluster solution, and the reaction was monitored via IR spectroscopy. The mixture was filtered, and the precipitate was washed with THF until the washings were colorless; 40 mL of 2-propanol were added dropwise, and the volume of the solvent was reduced in a vacuum. The black precipitate was collected by filtration, washed with several portions of 2-propanol and cyclohexane, and finally dried under reduced pressure. It was extracted


dx.doi.org/10.1021/ic302282y | Inorg. Chem. 2013, 52, 1960−1964

to a small Schlenk tube with a minimum amount of THF and cautiously layered with 2-propanol; well-shaped black crystals were obtained. $\nu$(CO) (THF): 2069w, 2038s, 1805w $cm^{-1}$. Yield: 120 mg (45%). Elem. anal. Found: C, 20.0; H, 1.65. Calcd: C, 18.55; H, 0.97.

**Crystal Structure Determination of $(NBu_4)2$ and 3.** The X-ray diffraction studies were carried out on a Bruker SMART 1K CCD area detector (Mo K$\alpha$ radiation, 50 kV and 30 mA generator settings). **2** is monoclinic $P2_1/m$ with $a$ = 15.5619(16) Å, $b$ = 21.250(2) Å, $c$ = 18.164(2) Å, $\beta$ = 91.633(3)°, and $V$ = 6004.2(11) $Å^3$. The final $R_1$ and $wR_2$ values were 0.0783 and 0.2389, respectively. **3** is also monoclinic, $P2_1/c$, with $a$ = 16.5865(6) Å, $b$ = 29.9739(10) Å, $c$ = 25.4375(9) Å, $\beta$ = 98.604(1)°, and $V$ = 12504.2(8) $Å^3$. The final $R_1$ and $wR_2$ values were 0.0731 and 0.2052, respectively. More details on data collection and crystal structure refinement are given in the Supporting Information.

## ■ ASSOCIATED CONTENT

### Supporting Information

Tables S1 and S2 (crystallographic data), ORTEP drawings of **2** and **3** with all atomic labels, and experimental details of crystallographic analysis. This material is available free of charge via the Internet at http://pubs.acs.org.

## ■ AUTHOR INFORMATION


### Corresponding Author

*E-mail: alessandro.ceriotti@unimi.it (A.C.), piero.macchi@dcb.unibe.ch (P.M.).


### Notes

The authors declare no competing financial interest.

## ■ ACKNOWLEDGMENTS

This paper was financially supported by MIUR [PRIN 2008 (to A.C. and F.F.d.B.) and PRIN 2007 (to R.D.P.)].

## ■ REFERENCES


(1) We found about 100 references in the CCDC database. Selected examples: (a) Bennett, M. A.; Berry, D. E.; Beveridge, K. A. *Inorg. Chem.* **1990**, *29*, 4148. (b) Braunstein, P.; Lehner, H.; Matt, D.; Tiripicchio, A.; Tiripicchio Camellini, M. *Angew. Chem., Int. Ed. Engl.* **1984**, *23*, 304. (c) Parish, R. V.; Moore, L. S.; Dens, A. J. J.; Mingos, D. M. P.; Sherman, D. J. *J. Chem. Soc., Dalton Trans.* **1989**, 539. (d) Briant, C. E.; Gilmour, D. I.; Mingos, D. M. P. *J. Chem. Soc., Dalton Trans.* **1986**, 835. (e) Manojlovic-Muir, L.; Muir, K. W.; Treurnicht, I.; Puddephatt, R. J. *Inorg. Chem.* **1987**, *26*, 2418. (f) Hallam, M. F.; Luke, M. A.; Mingos, D. M. P.; Williams, I. D. *J. Organomet. Chem.* **1987**, *325*, 271. (g) Mingos, D. M. P.; Oster, P.; Sherman, D. J. *J. Organomet. Chem.* **1987**, *320*, 257. (h) Hallam, M. F.; Mingos, D. M. P.; Adatia, T.; McPartlin, M. *J. Chem. Soc., Dalton Trans.* **1988**, 335. (i) Payne, N. C.; Ramachandran, R.; Schoettel, G.; Vittal, J. J.; Puddephatt, R. J. *Inorg. Chem.* **1991**, *30*, 4048. (l) Yip, J. H. K.; Jianguo, W.; Kwok-Yin, W.; Kam Piu, H.; So-Ngan Pun, C.; Vittal, J. J. *Organometallics* **2002**, *21*, 5292. (m) Imhof, D.; Burckhardt, U.; Dahmen, K.-H.; Ruegger, H.; Gerfin, T.; Gramlich, V. *Inorg. Chem.* **1993**, *32*, 5206. (n) Toronto, D. V.; Balch, A. L. *Inorg. Chem.* **1994**, *33*, 6132.

(2) (a) De Silva, N.; Dahl, L. F. *Inorg. Chem.* **2005**, *44*, 9604. (b) De Silva, N.; Laufenberg, J. W.; Dahl, L. F. *Chem. Commun.* **2006**, 4437. (c) Spivak, G. J.; Vittal, J. J.; Puddephatt, R. J. *Inorg. Chem.* **1998**, *37*, 5474.

(3) (a) Krogstad, D. A.; Young, V. G., Jr.; Pignolet, L. H. *Inorg. Chim. Acta* **1997**, *264*, 19. (b) Krogstad, D. A.; Konze, W. V.; Pignolet, L. H. *Inorg. Chem.* **1996**, *35*, 6763. (c) Breuer, M.; Strahle, J. *Z. Anorg. Allg. Chem.* **1993**, *619*, 1564. (d) Schoondergang, M. F. J.; Bour, J. J.; van Strijdonck, G. P. F.; Schlebos, P. P. J.; Bosman, W. P.; Smits, J. M. M.; Beurskens, P. T.; Steggerda, J. J. *Inorg. Chem.* **1991**, *30*, 2048. (e) Bour, J. J.; Schlebos, P. P. J.; Kanters, R. P. F.; Bosman, W. P.; Smits, J. M. M.; Beurskens, P. T.; Steggerda, J. J. *Inorg. Chim. Acta* **1990**, *171*, 177. (f) Ito, L. N.; Sweet, J. D.; Mueting, A. M.; Pignolet, L. H.; Schoondergang, M. F. J.; Steggerda, J. J. *Inorg. Chem.* **1989**, *28*, 3696. (g) Kanters, R. P. F.; Bour, J. J.; Schlebos, P. P. J.; Bosman, W. P.; Behm, H.; Steggerda, J. J.; Ito, L. N.; Pignolet, L. H. *Inorg. Chem.* **1989**, *28*, 2591. (h) Kanters, R. P. F.; Schlebos, P. P. J.; Bour, J. J.; Bosman, W. P.; Behm, H. J.; Steggerda, J. J. *Inorg. Chem.* **1988**, *27*, 4034. (i) Hallam, M. F.; Mingos, D. M. P.; Adatia, T.; McPartlin, M. *J. Chem. Soc., Dalton Trans.* **1988**, 335. (j) Bour, J. J.; Kanters, R. P. F.; Schlebos, P. P. J.; Bosman, W. P.; Behm, H.; Beurskens, P. T.; Steggerda, J. J. *Recl. Trav. Chim. Pays-Bas* **1987**, *106*, 157.

(4) (a) Behm, H. J.; Steggerda, J. J. *Inorg. Chem.* **1988**, *27*, 4034. (b) Bour, J. J.; Kanters, R. P. F.; Schlebos, P. P. J.; Steggerda, J. J. *Recl. Trav. Chim. Pays-Bas* **1988**, *107*, 211. (c) Kanters, R. P. F.; Bour, J. J.; Schlebos, P. P. J.; Bosman, W. P.; Behm, H.; Steggerda, J. J.; Ito, L. N.; Pignolet, L. H. *Inorg. Chem.* **1989**, *28*, 2591. (d) Ito, L. N.; Sweet, J. D.; Mueting, A. M.; Pignolet, L. H.; Schoondergang, M. F.; Steggerda, J. J. *Inorg. Chem.* **1989**, *28*, 3696.

(5) (a) Qian, L.; Yang, X. *J. Phys. Chem. B* **2006**, *110*, 16672. (b) Luo, J.; Njoki, P. N.; Wang, L.; Zhong, C. J. *Electrochem. Commun.* **2006**, *8*, 81. (c) Habrioux, A.; Vogel, W.; Guinel, M.; Guetaz, L.; Servat, K.; Kokoh, B.; Alonso-Vante, N. *Phys. Chem. Chem. Phys.* **2009**, *11*, 3573. (d) Mohamed, M. M.; Khairou, K. S. *J. Colloid Interface Sci.* **2011**, *354*, 100.

(6) (a) Villa, A.; Veith, G. M.; Prati, L. *Angew. Chem., Int. Ed.* **2010**, *49*, 4499. (b) Brett, G. L.; He, Q.; Hammond, C.; Miedziak, P. J.; Dimitratos, N.; Sankar, M.; Herzing, A. A.; Conte, M.; Lopez-Sanchez, J. A.; Kiely, C. J.; Knight, D. W.; Taylor, S. H.; Hutchings, G. J. *Angew. Chem., Int. Ed.* **2011**, *50*, 10136.

(7) Washecheck, D. M.; Wucherer, E. J.; Dahl, L. F.; Ceriotti, A.; Longoni, G.; Manassero, M.; Sansoni, M.; Chini, P. *J. Am. Chem. Soc.* **1979**, *101*, 6110.

(8) Ceriotti, A.; Masciocchi, N.; Macchi, P.; Longoni, G. *Angew. Chem., Int. Ed.* **1999**, *38*, 3724.

(9) Fedi, S.; Zanello, P.; Laschi, F.; Ceriotti, A.; El Afefey, S. *J. Solid State Electrochem.* **2009**, *13*, 1497.

(10) (a) Fumagalli, A.; Della Pergola, R.; Bonacina, F.; Garlaschelli, L.; Moret, M.; Sironi, A. *J. Am. Chem. Soc.* **1989**, *111*, 165. (b) Della Pergola, R.; Ceriotti, A.; Garlaschelli, L.; Demartin, F.; Manassero, M.; Masciocchi, N. *Inorg. Chem.* **1993**, *32*, 3349. (c) Femoni, C.; Iapalucci, M. C.; Longoni, G.; Tiozzo, C.; Zacchini, S.; Heaton, B. T.; Iggo, J. A.; Zanello, P.; Fedi, S.; Garland, M. V.; Li, C. *Dalton Trans.* **2009**, 2217.

(11) (a) Khimyak, T.; Johnson, B. F. G.; Hermans, S.; Bond, A. D. *Dalton Trans.* **2003**, 2651. (b) Gould, R. A. T.; Craighead, K. L.; Wiley, J. S.; Pignolet, L. H. *Inorg. Chem.* **1995**, *34*, 2902.

(12) (a) Fumagalli, A.; Martinengo, S.; Albano, V. G.; Braga, D.; Grepioni, F. *J. Chem. Soc., Dalton Trans.* **1989**, 2343. (b) Housecroft, C. E.; Matthews, D. M.; Waller, A.; Edwards, A. J.; Rheingold, A. L. *J. Chem. Soc., Dalton Trans.* **1993**, 3057. (c) Ceriotti, A.; Della Pergola, R.; Garlaschelli, L.; Manassero, M.; Masciocchi, N. *Organometallics* **1995**, *14*, 186.

(13) Shriver, D. F.; Drezdzon, M. A. *The Manipulation of air-sensitive compounds*, 2nd ed.; Wiley: New York, 1986.

(14) Bruce, M. I.; Nicholson, B. K.; Shawkataly, O. B. *Inorg. Synth.* **1989**, *26*, 325.